ELSEVIER

Ultramicroscopy 60 (1995) 295–309

ultramicroscopy

Diffuse scattering in electron diffraction data from protein crystals

N. Grigorieff, R. Henderson

MRC Laboratory of Molecular Biology, Hills Road, Cambridge CB2 2QH, UK

Received 26 January 1995; in final form 23 March 1995

Abstract

Diffuse background present in electron diffraction patterns from protein crystals can produce significant systematic error in intensity measurements. In certain regions of the diffraction pattern, this can even result in systematically negative intensity measurements. Thus, it is important to remove the diffuse background to produce more accurate measurement of structure factor amplitudes. The variable part of the continuous background arises from disorder in the crystal with an intensity which depends on the type of disorder. We show how the diffuse scattering can be calculated from a model for the disorder leading to a correction of intensities measured from diffraction patterns. For crystalline bacteriorhodopsin (bR) in native p3 ($a = 62.45$ Å) purple membrane the best correction for several models tested is obtained by assuming that the disorder comes from random displacement of the trimer of bR molecules as a rigid unit. The correction was applied to intensity measurements using improved error estimates based on the experimental errors. The number of intensities previously measured wrongly to be negative is about 10%. This is reduced by 4-fold to be in agreement with that expected from counting statistics. The final corrected amplitudes gave a lower R-factor when used for refinement of an atomic model.

1. Introduction

Accurate measurement of reflection intensities in electron diffraction patterns is of prime importance in the determination of the structure of a crystalline sample. Subsequent calculation and interpretation of the density map followed by model building all depends on the measured data. Therefore, it is necessary to study carefully sources of error and correct for them where possible.

The extraction of intensity data from photographic film starts with the densitometry on a scanner prior to computer processing [1]. Before integration of the spot intensity on the computer the background of inelastic scattering in the pattern is subtracted and the non-linearity of the film is corrected. The dominant part of the background comes from elastic and inelastic scattering from the carbon support film and any embedding medium, such as amorphous ice or glucose. It has a radially varying distribution and is determined as the average density at a given distance from the centre of the pattern excluding spots. Once this background is subtracted the remaining local background is determined for each spot separately by averaging the intensity surrounding the spot approximately midway between the spot and its nearest neighbours. This procedure assumes the local background varies linearly with position.

SSDI 0304-3991(95)00059-3

For 2-dimensional crystals of the p3 form of bacteriorhodopsin (bR, purple membrane) about 10% of the reflections sampled along z^* assuming the thickness of a unit cell is 100.9 Å, have negative intensities after subtraction of the background. This is significantly more than expected from error estimates suggesting a systematic error in the intensity data. The error directly affects the accuracy of structure factor amplitudes derived from the intensities which are used to calculate a density map. However, features in the map are much more sensitive to the phases which are measured independently from images. Hence, the systematic error in the measured diffraction intensities does not affect significantly the model built into the density map, and, therefore, it was ignored. However, in subsequent refinement of the model against the amplitudes the error has a larger effect and must be corrected. We show here that a better approximation of the background can be obtained from a calculation of diffuse scattering due to disorder in the crystal, and that a correction based on this approximation reduces the number of negative reflections to a number in keeping with that expected from error estimates.

The reflection intensities obtained from curve fits of lattice lines along z^* (see Section 4) are normally converted into amplitudes using the program TRUNCATE. The program is based on an algorithm proposed by French and Wilson [2], to provide a correct treatment of both positive and negative experimental intensity measurements. The program assumes that intensity measurements are affected only by random errors and, therefore, that for a weak spot the probability of a negative measurement after background subtraction depends only on the noise in the data. Therefore, the standard deviation for each measurement must be known accurately. Bayesian statistics are used to estimate the positive mean of the parent statistical distribution. The TRUNCATE algorithm is not able to correct for systematic errors due to diffuse background and the program normally discards measurements more negative than four standard deviations.

The present work focuses on modelling diffuse scattering from 2-dimensional crystals of the p3 form of bR and leads to a correction in the data published by Ceska and Henderson [3] and used by Henderson et al. [4] to produce an atomic model for the protein. A method for estimating standard deviations of intensities based on global fitting of the data is also described. These two improvements are then applied prior to further processing using TRUNCATE.

2. Estimation of the standard deviation in electron diffraction data

The standard deviation of a spot intensity measured from a diffraction pattern could be deduced from a sufficiently large number of independent measurements. This is not a feasible approach in biological electron microscopy or diffraction since multiple exposure of the same sample is not possible due to beam damage and the diffraction patterns from two crystals always differ due to slight differences in orientation. Thus, it is necessary to obtain error estimates based on counting statistics and the overall quality of the data set. To a first approximation the standard deviation σ in an intensity measurement is given by counting statistics from the number of electrons in a particular reflection. For the intensity I given by the number of electrons in a particular measurement we have:

$$\sigma(I) = \sqrt{I}\,. \tag{1}$$

In X-ray diffraction the estimate of the error is often obtained by fitting an averaged profile to each spot. The fit is done by least squares and yields an error for the profile scale factor and, hence, intensity which is based on the standard deviation of the measurements at each pixel contributing to the profile. If there are symmetry-related reflections the estimate can be improved further by comparing the independent measurements of the same diffraction peak.

In electron diffraction a simpler method has been used which estimates the error in measurement of a particular pair of reflections as the difference between the Friedel mates. The curvature of the Ewald sphere and dynamical (multiple) scattering cause Friedel-related reflections to

have different intensities and, therefore, lead to an overestimate of the error in a measurement. Both of these effects should be small, however [5]. The error from a Friedel pair difference relies on only two measurements for each reflection and may lead to unrealistically high or low error estimates if it is used directly. An improved estimate can be obtained from the measurements by determining a set of parameters which describe the standard deviation for each reflection in the whole data set. The parameters were chosen to be intensity I (cf. Eq. (1)) and reciprocal space coordinate z^* (perpendicular to the plane of the 2-dimensional crystal). The coordinate z^* of diffraction spots increases with the specimen tilt angle and corresponding spots are more blurred due to slight sample buckling (lack of perfect flatness). The variance of the measured intensity of a blurred spot thus increases with the area occupied by the spot due to noise in the underlying film background. The area is roughly proportional to z^{*2} and we may write for the calculated variance σ_c^2 of a spot intensity:

$$\sigma_c^2(I, z^*) = r_1 + r_2 I + r_3 z^{*2} + r_4 I z^{*2}, \qquad (2)$$

where r_1 to r_4 are constants which can be determined from a least-squares fit of the function Eq. (2) to the observed variance $\sigma_{obs}^2(I, z^*)$. A weighting factor, r_k, for a particular film k may be introduced to give the final new estimate for the variance:

$$\sigma_{new}^2(I, z^*, k) = r_k \sigma_c^2(I, z^*). \qquad (3)$$

The weighting factor allows for variations in the strength and quality of each diffraction pattern and is calculated as:

$$r_k = \frac{\sigma_k}{\bar{\sigma}_k}, \qquad (4)$$

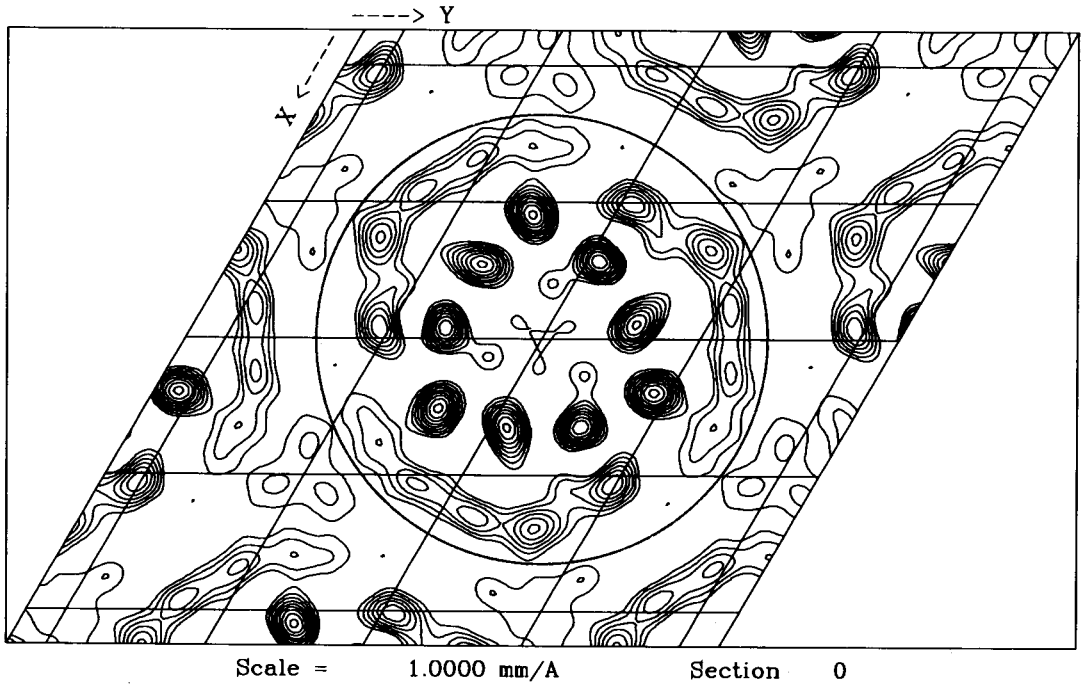

Fig. 1. Projection map of the native p3 form of bacteriorhodopsin at 6 Å resolution. The extent of the protein trimer is indicated by a surrounding circle.

with

$$\sigma_k = \sqrt{\frac{\sum_{\substack{\text{all reflections}\\ \text{on film } k}} \sigma_{\text{obs}}^2/\sigma_c^2}{n-1}}, \qquad (5)$$

where n is the number of reflections on film k and σ_k may be interpreted as a relative standard deviation of intensities on film k. $\bar{\sigma}_k$ is the average over all films.

3. Diffuse scattering from partially disordered crystals

Coherent elastic electron diffraction into discrete spots is always accompanied by diffuse background. This is partially due to inelastic scattering in the sample, such as scattering by plasmons, core losses and, in some cases, thermal diffuse scattering (phonon scattering). In biological specimens, a major contribution originates from frozen-in disorder in the crystal. These are small displacements of molecules and atoms within molecules from their positions given by the underlying lattice and the average structure, respectively. When the specimen is held at liquid nitrogen temperatures the displacements are static and random. In native bR the molecules are arranged in closely packed trimers surrounded by lipids which are more mobile (see Fig. 1). The trimers have, therefore, some degree of freedom to be displaced in the crystal plane. Monomers are more restricted in their displacement relative to the trimer due to the close packing of the trimer. The displacement of adjacent trimers is uncorrelated if there are no cracks in the crystal and the displacements are small relative to the gap between trimers. In this case, we may assume an isotropic Gaussian distribution for the displacement vectors in the plane of the crystal. The displacement vectors perpendicular to the crystal are likely to be smaller due to restraints by the supporting carbon film, but could be of a similar magnitude in the 1–2 Å region. Preliminary results from crystallographic refinement against an atomic model suggests the intrinsic order parallel and perpendicular to the membrane is similar.

A comprehensive review of diffuse scattering of X-rays and neutrons by partially disordered crystals is given by Jagodzinski and Frey [6] and Benoit and Doucet [7]. The results are also applicable to electron scattering. The distribution of the diffuse intensity depends on the nature of the disorder. If the molecules are well ordered and only the atoms within each molecule deviate from their average position the diffuse background will be constant for a given scattering angle. The situation changes if groups of atoms are displaced as a rigid unit. In bR we may expect that, apart from the intramolecular displacement of individual atoms, the trimer and perhaps part of the lipids are displaced as one unit. The diffuse background is then given by the scattering of this unit, i.e. the molecular transform of the trimer, and the distribution is no longer isotropic. To subtract the background accurately from the spot intensity it would have to be measured close to each spot. This is normally done with X-ray diffraction patterns where spots are stronger because the crystals are very big. In electron diffraction patterns from 2-dimensional crystals the spots are weaker and blurred in tilted specimens if the sample is not perfectly flat. Generally, the crystals are limited in size and large areas of background must be measured between spots to increase the accuracy with which the background is measured. Similarly in data from tilted specimens, spot blurring also means that the background must be measured well away from the spot centre, e.g. halfway between two spots. For a spot located at a background minimum this will give an overestimate of the background. Likewise, the background is underestimated for a spot at a maximum in the diffuse background. The error affects both weak and strong reflections and will increase the noise in the density map calculated from amplitudes based on the background-corrected intensities. A more accurate model for the diffuse background will, therefore, improve the density map and models derived from it, and lead to a better refinement of the model against the corrected amplitudes.

3.1. Calculation of the diffuse background from an atomic model

The average structure factor $F_0(\boldsymbol{q})$ for a crystal with disorder is given by:

$$F_0(\boldsymbol{q}) = \sum_i f_i(q)\,\exp(-2\pi i \boldsymbol{q}\cdot\boldsymbol{r}_i)\,\exp\left(-B_i q^2/4\right), \tag{6}$$

where the sum runs over all atoms i in one unit cell. $f_i(q)$, $\boldsymbol{r}_i$ and B_i are the form factor, coordinate and temperature factor for atom i, respectively, and q is the modulus of the scattering vector $\boldsymbol{q}$. If groups of atoms within the unit cell are displaced as rigid units we may write the structure factor $F_0(\boldsymbol{q})$ as a sum of structure factors $F_j(\boldsymbol{q})$ for each group:

$$F_0(\boldsymbol{q}) = \sum_j F_j(\boldsymbol{q})\,\exp\left(-B_j^{\mathrm{G}} q^2/4\right), \tag{7}$$

with

$$F_j(\boldsymbol{q}) = \sum_{i\in\text{group } j} f_i(q)\,\exp(-2\pi i \boldsymbol{q}\cdot\boldsymbol{r}_i) \times \exp\left(-B_{j,i} q^2/4\right), \tag{8}$$

where B_j^{G} and $B_{j,i}$ are the temperature factors for group j and atom i within group j, respectively. For simplicity we have assumed the displacement of the rigid units is isotropic and can be described by scalar temperature factors. This seems to be true for bR (see Section 4). Thus, the displacement of atoms in each group is the sum of displacements of the group as a whole and atoms relative to it, and $B_i = B_j^{\mathrm{G}} + B_{j,i}$. The attenuation of the structure factor for each group at higher resolution depends on the temperature factors $B_{j,i}$. Even if the overall structure factor $F_0(\boldsymbol{q})$ is attenuated by groups being displaced relative to each other individual groups may still scatter coherently. Coherent scattering from a randomly displaced group results in diffuse background with a modulation given by the structure factor of the group. The amount of diffuse scattering depends on the resolution. Using the Patterson function approach [8] we find for the diffuse intensity $I_{\mathrm{d}}(\boldsymbol{q})$:

$$I_{\mathrm{d}}(\boldsymbol{q}) = \sum_j \left(1-\exp\left[-B_j^{\mathrm{G}} q^2/2\right]\right)\left|F_j(\boldsymbol{q})^2\right| + \sum_j \sum_{i\in\text{group } j} \left(1-\exp\left[-B_{j,i} q^2/2\right]\right) f_i^2(q). \tag{9}$$

In Eq. (9) we assumed all groups are displaced independently of each other. This is a good approximation for displacements small enough to be unrestrained by adjacent groups.

The second term in Eq. (9) includes incoherent scattering from individual atoms which is isotropically distributed around the central beam. As described above, this part of the background is subtracted correctly and can, therefore, be ignored in the following discussion. The first term in Eq. (9) describes the modulated diffuse background from groups of atoms. During processing of a diffraction pattern on the computer the background found approximately halfway between spots is subtracted from the spot intensity. The error $I_{\mathrm{e}}(\boldsymbol{g})$ for a spot at $\boldsymbol{q}=\boldsymbol{g}$ made according to Eq. (9) is thus:

$$I_{\mathrm{e}}(\boldsymbol{g}) = I_{\mathrm{d}}(\boldsymbol{g}) - \overline{I_{\mathrm{d}}(\boldsymbol{g}+\boldsymbol{q}_p)}, \tag{10}$$

with

$$I_{\mathrm{d}}(\boldsymbol{g}) = \sum_j \left(1-\exp\left[-B_j^{\mathrm{G}} g^2/2\right]\right)\left|F_j(\boldsymbol{g})\right|^2. \tag{11}$$

$\overline{I_{\mathrm{d}}(\boldsymbol{g}+\boldsymbol{q}_p)}$ signifies the average diffuse scattering power between spots with p the fraction of the distance to nearest neighbour spots. In our case $p = 0.5$.

If the sample is not flat, spots will be blurred and density is spread over a bigger area. Thus, spot intensities have to be integrated over a larger area. This causes an increase in the contribution of the diffuse scattering to the experimental measurement because the blurring increases with the reciprocal space coordinate z^* perpendicular to the sample plane. If $A(z^*)$ is the area at z^* over which to integrate the spot, the diffuse background contribution to the integrated intensity is $A(z^*)I_{\mathrm{d}}(g)$. The contribution of diffuse back-

ground which is subtracted from the integrated intensity is $A(z^*)\overline{I_d(\boldsymbol{g}+\boldsymbol{q}_p)}$ and, hence,

$$I_{obs}(\boldsymbol{g}) = I_0(\boldsymbol{g}) + A(z^*)\left[I_d(\boldsymbol{g}) - \overline{I_d(\boldsymbol{g}+\boldsymbol{q}_p)}\right], \tag{12}$$

where $I_{obs}(\boldsymbol{g})$ and $I_0(\boldsymbol{g})$ are the observed and true spot intensities, respectively. To arrive at the corrected intensity $I_{new}(\boldsymbol{g})$ we therefore have:

$$I_{new}(\boldsymbol{g}) = I_{obs}(\boldsymbol{g}) + I_c(\boldsymbol{g}), \tag{13}$$

with

$$I_c(\boldsymbol{g}) = A(z^*)\left[\overline{I_d(\boldsymbol{g}+\boldsymbol{q}_p)} - I_d(\boldsymbol{g})\right]. \tag{14}$$

In the case of bR (Section 4) it was found empirically that $A(z^*)$ is approximately given by:

$$A(z^*) = c_1(1 + c_2 z^*), \tag{15}$$

with c_1 and c_2 constants. These constants and the temperature factors B_j^G (Eq. (11)) are determined as follows. A correlation coefficient L_{obs} can be calculated between observed negative intensities $I_{obs}(\boldsymbol{g})$ and corrections $I_c(\boldsymbol{g})$,

$$L_{obs} = \frac{\sum_{I,\text{negative}} I_{obs}(\boldsymbol{g}) I_c(\boldsymbol{g})}{\sum_{I,\text{negative}} |I_{obs}(\boldsymbol{g}) I_c(\boldsymbol{g})|}. \tag{16}$$

The correlation coefficient, L_{obs} indicates how well the model for the rigid units accounts for the background. A perfect model should give $L_{obs} \approx -1.0$. We may define another correlation coefficient L_{new} for the corrected intensities $I_{new}(\boldsymbol{g})$. Once the diffuse background has been removed the remaining negative reflections should be uncorrelated with $I_c(\boldsymbol{g})$, and L_{new} should be zero. Another measure for a successful correction is a reduction in the number of remaining negative reflections. These can be quantified by a ratio M where:

$$M = \frac{\sum_{I,\text{negative}} I_{new}(\boldsymbol{g})}{\sum_{I,\text{positive}} I_{new}(\boldsymbol{g})}. \tag{17}$$

The correct model for the rigid units should minimise M. The constants c_1, c_2 and the temperature factors B_j^G are chosen to minimise $|L_{new}| + |M|$.

The sum over all corrections $I_c(\boldsymbol{g})$ should be small as corrections for weak and strong reflections should be of opposite sign and cancel. The sum over $I_c(\boldsymbol{g})$ can be given as percentage S of the average absolute value of $I_c(\boldsymbol{g})$ which can be used as a check that the behaviour is correct:

$$S = \frac{\sum_{\text{all reflections}} I_c(\boldsymbol{g})}{\sum_{\text{all reflections}} |I_c(\boldsymbol{g})|}. \tag{18}$$

After correction of intensities for diffuse scattering and estimation of new standard deviations for each measurement (see Section 2) a statistical target N_s for the number of remaining negative reflections N can also be calculated as:

$$N_s = 0.5 \sum_{\text{all reflections}} \operatorname{erfc}\left(\frac{|F_{new}(\boldsymbol{g})|^2}{\sqrt{2}\,\sigma_{new}}\right), \tag{19}$$

where erfc is the complementary error function, $F_{new}(\boldsymbol{g})$ are the structure factors calculated from the background-corrected intensities and σ_{new} are the estimates of standard deviations of reflection intensities given in Section 2.

3.2. Calculation of the diffuse background from a density map

In Eq. (6) it is assumed that the atomic structure of the crystal is accurately known. In most cases the resolution obtained from electron microscopy of 2-dimensional protein crystals does not allow model building and even if the resolution is sufficiently high for interpretation at the atomic level the model usually shows disagreement with the measured data at an R-factor of 25 to 30%, at least for the very small number (two) of structures so far examined. Calculating a correction from a model which is later added or subtracted from the measured data may also introduce a bias for or against the model leading to spurious results in later refinement. Also, as will be seen later, the inaccuracy of the model may result in poor correction of the data. It is thus desirable to calculate the diffuse background directly from the map calculated from the observed data.

Table 1
Complete reflection file for bacteriorhodopsin and reset standard deviations after curve fitting

Resolution (Å)	Number of independent reflections measured	Number of films	Number of standard deviations reset
2.5	58457	150	39016

To do this we start by assuming the measured data has no diffuse background component in it and leads to structure factors $F_0(\boldsymbol{g})$ given by Eq. (6). We further assume that apart from the intensities we also have phases for all reflections in the resolution range considered. This means we can calculate a 3-dimensional density map to use instead of an atomic model. To get the structure factors of a particular rigid unit we have to isolate the unit by masking off the remaining density in the map. More specifically, we start with a map $\rho(\boldsymbol{r})$ which is the inverse Fourier transformation of a set of structure factors $F_0(\boldsymbol{g})$ as given by Eq. (6). To get the density $\rho_j(\boldsymbol{r})$ of a rigid unit j we cut out some density by multiplication with a shape function $s(\boldsymbol{r})$ describing the envelope of the rigid unit:

$$\rho_j(\boldsymbol{r}) = \rho(\boldsymbol{r}) s(\boldsymbol{r}). \tag{20}$$

A forward Fourier transform will then give the structure factors of rigid unit j (cf. Eq. (8)).

$$F_j(\boldsymbol{q}) = [(F_0 * s)(\boldsymbol{q})] \exp\left(B_j^{\mathrm{G}} q^2/4\right). \tag{21}$$

The $*$ signifies a convolution and $s(\boldsymbol{q})$ is the shape transform of the rigid unit. The exponential compensates for the attenuation of $F_0(\boldsymbol{g})$ caused by random displacement of rigid unit j.

Table 2
Least-squares fit parameters for $\sigma^2 = r_1 + r_2 I + r_3 z^{*2} + r_4 I z^{*2}$, resulting R-factor and linear correlation between data and fit for different combinations of parameters

Parameters used in fit	R-factor	Linear correlation
r_1	0.96	0.0
r_2	0.84	0.51
r_3	0.84	−0.10
r_1, r_2	0.69	0.52
r_1, r_3	0.95	0.07
r_1, r_2, r_3	0.69	0.52
r_1, r_2, r_3, r_4	0.68	0.52

The convolution with $s(\boldsymbol{q})$ causes interference between reflections. If the rigid unit is comparable in size with that of the unit cell the power of $s(\boldsymbol{q})$ concentrates around $\boldsymbol{q} = 0$ and will be small beyond the nearest neighbour spots. This means that interference is mainly between adjacent reflections and higher orders can be neglected in the evaluation of Eq. (21).

The ideal structure factors are not known and we have to use the observed structure factors $F_{\mathrm{obs}}(\boldsymbol{g})$ as a first approximation. Thus, using Eqs. (11), (14) and (21) we finally have:

$$I_{\mathrm{new}}(\boldsymbol{g}) = I_{\mathrm{obs}}(\boldsymbol{g}) + A(z^*) \sum_j \left[\exp\left(B_j^{\mathrm{G}} g^2/2\right) - 1\right] \times \left[\overline{\left|(F_{\mathrm{obs}} * s_j)(\boldsymbol{q}_p)\right|^2} - \left|(F_{\mathrm{obs}} * s_j)(\boldsymbol{g})\right|^2\right]. \tag{22}$$

$\overline{|(F_{\mathrm{obs}} * s_j)(\boldsymbol{q}_p)|^2}$ signifies the average diffuse scattering power between spots, as before. Phase information usually does not extend to resolution as high as for amplitudes. If the phase relation in a pair of adjacent reflections is unknown we have

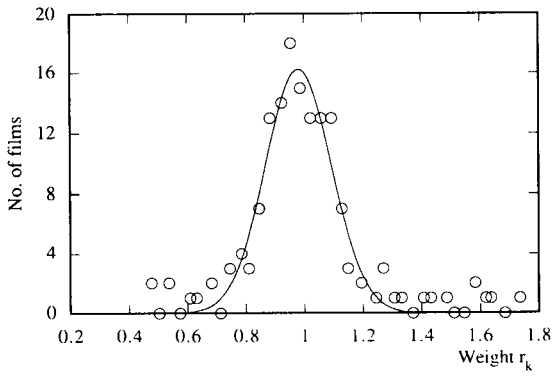

Fig. 2. Distribution of film weighting factors r_k for all films (total = 150). The line is a least-squares fit of a Gaussian.

to take the average intensity for a random distribution of phases which is equivalent to adding the intensities of both reflections at point q_p.

The background between spots in a particular diffraction pattern should be calculated at points lying in the plane of the diffraction pattern each one of which represents a central section through the 3-dimensional transform. The intensities of spots from each diffraction pattern are merged to create the sampling along lattice lines of particular h and k indices. This produces more reliable intensities. However, the orientation of planes of individual patterns cannot easily be retrieved from the merged data. The background is therefore calculated in planes perpendicular to z^*. This is a good approximation for tilt angles of up to 60° and for thin crystals where the intensity of the lattice lines does not vary rapidly.

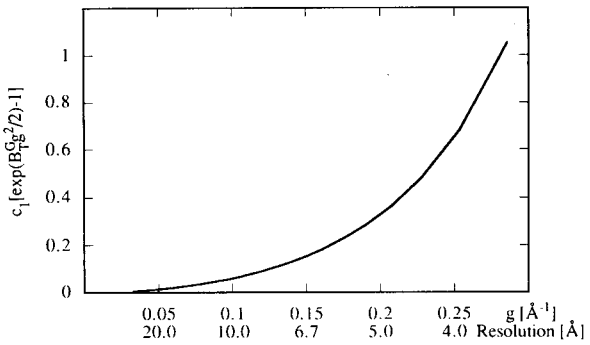

Fig. 3. Scale factor $c_1[\exp(B_T^G g^2/2)-1]$ for the diffuse background calculated from the density map assuming the trimer without lipids as a rigid unit. The scale factor $c_1 = 0.29$ and the temperature factor for the trimer, $B_T^G = 16$ Å^2 (see Table 3).

4. Results for bacteriorhodopsin

New estimates for the standard deviations of intensities measured from diffraction patterns where calculated for bacteriorhodopsin using the procedure described in Section 2. The results are summarised in Tables 1 and 2. A fit using only parameters r_1 and r_2 gave a high correlation with the error estimates. Further terms in Eq. (2) did not improve the fit and were omitted. The distribution of film weighting factors r_k is shown in Fig. 2 and resembles approximately a Gaussian with a standard deviation of 0.16 indicating that most films were of approximately equal quality.

Lattice lines were fitted to the complete set of measured intensities using the program SYNCFIT [9] and a list of indexed reflections and errors based on the curve fit was obtained. In this initial curve fitting 363 out of 4753 reflections were negative. The intensities to 3.5 Å resolution

Table 3
Results for the correction of diffuse background assuming different models for the rigid units

Rigid Units	3 monomers (atomic model)	Trimer (atomic model)	Trimer and lipids (density map)	Trimer (density map)
Resolution of intensity data	3.5 Å	3.5 Å	3.5 Å	3.5 Å
Number of reflections	4753	4753	4753	4753
Number of phases	4753	4753	3766	3766
Negative reflections at start	363	363	363	363
Correlation L_{obs}	−0.45	−0.68	−0.85	−0.97
Correlation L_{new}	0.00	0.00	0.00	0.00
Sum of all corrections S	−0.17	−0.26	−0.64	0.03
Remaining negative reflections	346	322	269	94
Rigid unit temperature factor	$B_M^G = 19$ Å^2	$B_T^G = 4$ Å^2	$B_T^G = 8$ Å^2	$B_T^G = 16$ Å^2
Overall scale c_1	0.25	1.13	0.76	0.29
z^* scale c_2	8.32	9.75	28.59	37.53

The rigid unit temperature factor B_T^G should be compared to the overall temperature factor for the atomic model at 18 Å^2, reflecting both the displacement of rigid units and atoms within them. The statistical target N_s of remaining negative reflections calculated using intensities with improved error estimates and corrected for diffuse background was 70 which is close to the number actually achieved using the trimer without lipids from the density map as a rigid unit.

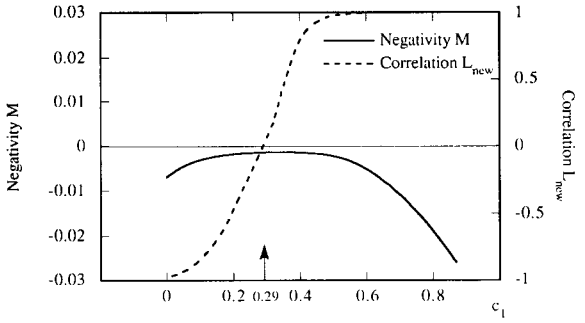

Fig. 4. Ratio of the sum of negative and positive reflections, M, and correlation coefficient, L_{new}, after application of the diffuse scattering correction with variable scale factor c_1. The optimum scale factor $c_1 = 0.29$ (see Table 3) found by minimising $|L_{new}| + |M|$ is marked by an arrow.

were then corrected for diffuse scattering. The tightly packed trimeric arrangement of bR in native purple membrane separated by a surrounding ring of lipid molecules (see Fig. 1) suggests the protein trimer behaves as a rigid unit (see Section 3). In this case there is only one temperature factor, $B_1^G = B_T^G$, for the trimer (Eq. (7)). Depending on strength of the lipid–protein and the protein–protein interactions possible alternative choices of rigid units might be a protein trimer including the adjacent ring of lipids or three separate protein monomers being displaced independently. The temperature factors for each monomer must be equal for symmetry reasons, and $B_1^G = B_2^G = B_3^G = B_M^G$.

The diffuse background for three monomers and a trimer was calculated using a version of the atomic model for bacteriorhodopsin derived by further refinement from that published by Henderson et al. [4]. The model had an overall R-factor of 25% and a phase residual of 66° compared to still noisy experimental phases measured independently from images. It was assumed that the displacement of the rigid units is isotropic because the overall temperature factor for the atomic model was found to be approximately the same in every direction. Both models for the rigid units, when used to derive a diffuse scattering correction, lead to a reduction in the number of reflections with negative intensities. However, the values for the correlation, L_{obs}, between observed negative reflections and corrections, and the number, N, of remaining negative reflections clearly identify the trimer as the more correct model (see Table 3). However, neither model meets the statistical target $N_s = 70$ for remaining negative reflections. In the last two columns, the experimental density map was used to calculate the background, as described in Section 3.2, both for a trimer including lipids and for a trimer without lipids. Despite some missing phase information the correlation, L_{obs}, between observed negative intensities and corrections is then much higher (89% and 97%). The correction derived from the trimer including lipids reduces the number of negative reflections further but the best

Table 4
Negative reflections before and after correction for diffuse background, divided into resolution zones, the statistical target value of remaining negatives and the average correction relative to the original intensities

Resolution	Number of reflections	Negative I_{obs}	Negative I_{new}	Target N_s	Average correction
27.0–10.3	170	0	0	1	1%
10.3–7.6	289	7	5	3	2%
7.6–6.3	355	9	6	4	6%
6.3–5.5	426	17	4	4	10%
5.5–4.9	467	19	4	2	17%
4.9–4.5	524	38	5	3	27%
4.5–4.2	577	50	8	5	30%
4.2–3.9	612	49	7	6	32%
3.9–3.7	644	69	18	14	37%
3.7–3.5	689	105	37	28	32%
27.0–3.5	4753	363	94	70	18%

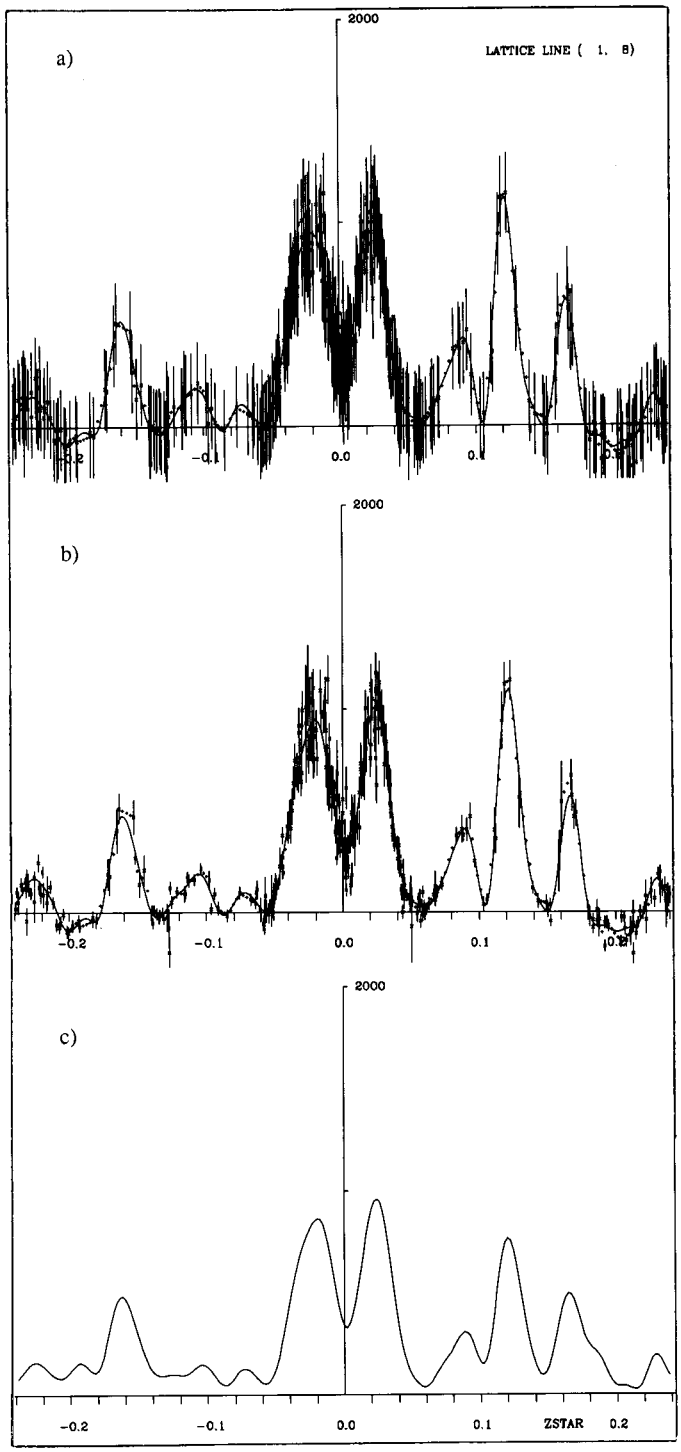

Fig. 5. Two examples of lattice lines at different stages of improvement. Lattice line (1, 8) is shown in its original state in (a), with new standard deviations in (b), and corrected for diffuse scattering in (c). Plots (d)–(f) show the same stages for lattice line (2, 6).

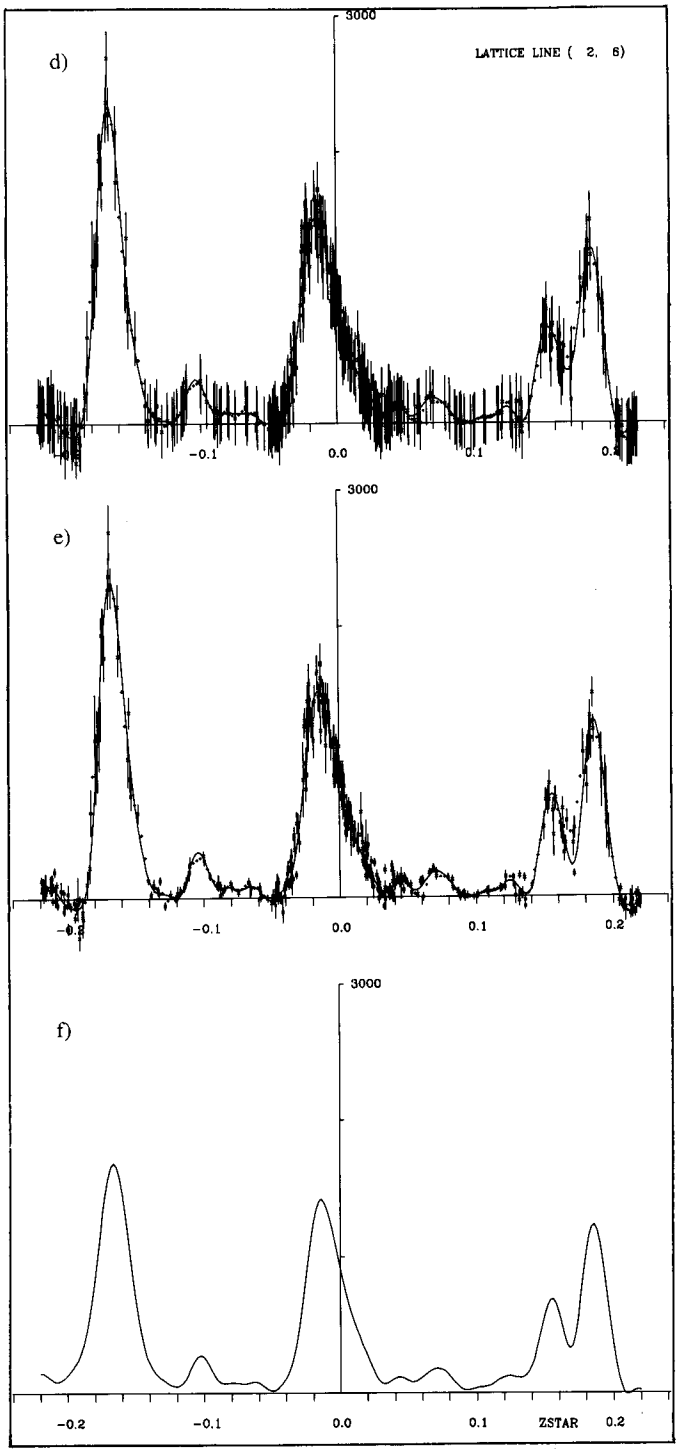

Fig. 5 (continued).

result of all was obtained for a trimer without lipids. The number of remaining negative reflections for this model was 94 which is close to the statistical target. This suggests the outer lipids are not displaced coherently with the trimer. The result also fits well with how the crystal components pack and repack, for example, in other crystal forms [10] where the trimer behaves as a rigid unit relative to the lipids and the neighbouring trimers. It might also be expected that when the trimer is displaced, the lipids move out of the way like a liquid. The improvement of the correction based on the density map over that based on the atomic model is likely to be due to the inaccuracy of the model. The temperature factor B_T^G at 16 Å^2 for the trimer is in good agreement with the overall temperature factor for the atomic model (18 Å^2) which should be an upper limit. A plot of the scale factor for the diffuse background in Fig. 3 and the average correction for a particular resolution zone in Table 4 show that the background correction is small at a resolution below 10 Å and increases rapidly beyond 4.5 Å resolution to about 30%.

Fig. 4 shows how the correlation coefficient, L_{new}, and the ratio of the sum of negative and positive reflections, M, change with the overall scale factor c_1. Similar plots may be obtained for the scale factor c_2 and the temperature factor B_T^G. L_{new} is a steep function of c_1 and the intercept at $L_{new} = 0$ determines c_1 accurately. The number of remaining negative reflections represented by the ratio M has a minimum close to the intercept at $L_{new} = 0$ and does not change much in the vicinity of its minimum. This means that a small increase in c_1 further removes reflections which were previously negative and causes an approximately equal number of positive reflections to become negative. A small decrease in c_1 has the opposite effect.

As an example of a lattice line with large negative regions the lattice line $(h, k) = (1, 8)$ is shown in its original state [4] in Fig. 5a, with new standard deviations in Fig. 5b and corrected for diffuse scattering in Fig. 5c. In the first plot the error bars are those measured from the Friedel pair differences but with errors below a given value reset to that value to avoid singularity of the least squares fit matrix for Friedel pairs accidentally measured as zero or close to zero. The principal difference between the first and second plot lies, therefore, in regions where standard deviations are small and mainly in regions of small intensity. The new standard deviations do not change the lattice line fit significantly. Their main effect comes into play when the intensities are subsequently converted to amplitudes using the program TRUNCATE. Negative intensities frequently occur at about $z^* = 0.2$ Å^{-1} in both plots. These are completely removed in the third plot which also shows changed peak envelopes and intensities. The plot suggests that the background correction tends to increase small intensities whereas large intensities are decreased. This is a consequence of the nature of the background. The background in weak reflections measured as the intensity between spots is generally an overestimate due to spillage of intensity from adjacent strong reflections, and the background correction will be an addition of intensity. The background in a strong reflection peaks approximately at the position of the spot and falls to a smaller value on the way to adjacent weaker spots. The background estimate from the interstitial intensity is, therefore, likely to be too small for strong reflections, and the correction will be a reduction.

In Figs. 5d–5f a second lattice line, $(h, k) = (2, 6)$, is shown with fewer negative regions, at different stages of processing analogous to Figs. 5a–5c. Small intensities remain approximately the same and are close to zero. As in the first example, all negative regions were removed by the correction. Lattice line (2, 6) is a typical curve where the minima are conserved after the diffuse background correction. Overall, it is clear that this diffuse scattering correction represents a significant change in the estimated structure factors.

As shown by Wilson [11] the distribution of reflection intensities is sensitive to the crystal symmetry. A ratio ρ can be defined as:

$$\rho = \frac{|\bar{F}|^2}{\bar{I}}, \tag{23}$$

with $|\bar{F}|$ and $\bar{I}$ the average structure factor amplitude and the average reflection intensity, re-

spectively. Assuming a uniform distribution of atoms in the unit cell $\rho_c = 0.637$ for a crystal with a centre of inversion (centric) and $\rho_a = 0.785$ for a crystal with no centre of inversion (acentric). The p3 crystal form of bR in native purple membrane is acentric. The atoms are not uniformly distributed but the structure mainly consists of helices. Thus, the intensity distribution may deviate from Wilson statistics. ρ_{bR} was estimated from the atomic model used in Section 4 to calculate the diffuse scattering correction, and it was found that $\rho_{bR} = 0.737$. For the original reflection intensities I_{obs}, $\rho_{obs} = 0.703$. Here, the structure factors were taken as the square root of the intensities (negative reflections were excluded). Similarly, for the corrected data, I_{new}, a value $\rho_{new} = 0.742$ was obtained which matches very closely the target value ρ_{bR} from the atomic model and is also closer to the theoretical value for an acentric random atom structure.

To check that the final improvement in the data could also be observed from an entirely different type of calculation, an initial atomic model built into the experimental density map but without any refinement and having an initial *R*-factor of about 47% was refined in 200 cycles of Hendrickson–Konnert refinement using uncorrected and corrected structure factors. The final *R*-factors were 30.60% and 30.20%, respectively.

5. Discussion

The high correlation of positive corrections with negative intensities and the 4-fold reduction of the number of negative reflections strongly support the model we use for the diffuse background. As shown in Table 4 the difference between the number of reflections with negative intensities after correction and the statistical target is negligible up to 3.9 Å and goes up only in the last two resolution zones. Several assumptions were made in the calculation of the correction which could lead to remaining minor discrepancies. First, in Eq. (22) the true structure factors were approximated by their observed values including errors due to inaccurate estimates of standard deviations and diffuse scattering. At higher resolution the diffuse background becomes stronger while the measured intensities are weaker. This causes an increase in the noise as well as a larger deviation of the observed structure factors from their true values, making the approximation in Eq. (22) worse. The incorporation of improved standard deviations in the observed structure factors before correction of the diffuse background is not possible since the smaller errors (see Fig. 4) cause rejection of most negative reflections when converting intensities to amplitudes using TRUNCATE. This is because the rejected reflections are much more negative than expected from their improved errors, due to the systematic error we are intending to remove.

A further source of error is due to the position at which we calculate the interstitial background. As pointed out in Section 3 the interstitial positions were taken to be at the same z^* coordinate as the spots being considered. Experimental diffraction patterns are sections through reciprocal space at an angle equal to the tilt angle of the crystal. The correct interstitial positions would, therefore, lie at z^* coordinates above and below the spot.

Third, not all phases to 3.5 Å are known from experiment (see Table 3) and a further approximation must be used. This leads to additional errors in the diffuse background calculated from the experimental data. With a more accurate atomic model for bR missing phases could be replaced by those calculated from the model. Calculation of the entire diffuse background (amplitudes and phases) will give a better correction than that calculated using the density map if the atomic model is sufficiently accurate and has been refined against a different set of data. If the background is calculated from a model with a certain *R*-factor against the observed data which we aim to correct, the correction is likely to increase the *R*-factor. This is because in Eq. (14), the intensity calculated at the spot, $I_d(\boldsymbol{g})$, is subtracted from the observed intensity. Since the square root of $I_d(\boldsymbol{g})$ matches exactly the structure factor amplitudes from the model subtraction of $I_d(\boldsymbol{g})$ selectively removes a fraction of the data which is in agreement with the model leading to

an increased R-factor. Using a model derived from and refined against a different data set will not have this bias.

Finally, the trimers have been assumed to be randomly displaced (see Section 3.1). For large displacements this assumption might not be valid, even with negligible protein–lipid interaction, because adjacent trimers will constrain the maximum distance of displacement to that given by the averaged distance of trimers visible in the projection map in Fig. 1, i.e. to about 6 Å. A quick calculation shows that the RMS value of the random displacement Δ with mean square value $\overline{\Delta^2}$ giving rise to the temperature factor $B_T^G = 8\pi^2\overline{\Delta^2}$ is 0.44 Å for $B_T^G = 16$ Å^2. This is compatible with the concept of independent displacement of the trimers and no inaccuracy in the calculated background should arise from this assumption.

An improved correction for the diffuse scattering could be calculated from the corrected structure factor amplitudes that have been derived from intensity data using improved error estimates and corrected for diffuse scattering using the initial amplitudes. This would be a second cycle of correction leading to an iterative procedure which could deal also with larger initial deviations of the observed amplitudes from their true values. Indeed, the number of negative reflections is further reduced in a second cycle (not shown here). However, possible inaccuracies in the calculated background other than those due to errors in the observed amplitudes, as described in the preceding paragraphs, might be amplified during the iteration, and, therefore, we regard the correction after the first cycle as a safe compromise between the improvements in later cycles and possible amplification of errors.

A correction of diffuse background in diffraction data arising from disorder in the crystal can ba calculated for other crystals provided the displacement of the atoms in the crystal occurs collectively in rigid units. The likely rigid units might be selected by inspection of the density map. Alternatively, correlated displacement of atoms in a crystal may be predicted by analysis of normal vibrational modes or molecular dynamics simulations [7]. Since protein molecules are likely to be displaced approximately as rigid units and, depending on the strength of the protein–protein contacts, several molecules might be included in one unit. In the p3 form of purple membrane, apart from the tight arrangement of bR molecules in a trimer visible in the projection map (Fig. 1) the strong binding between the monomers in the trimer is evident from a different crystal form where 80% of the lipids were removed upon treatment with sodium deoxycholate [10]. In these crystals the trimer structure was conserved with no observable modification of the bonding between the monomers. A few remaining lipids were located in the middle of the trimer suggesting they are not easily separable from the trimer and, therefore, are part of the rigid unit. In crystals where more than one distinct rigid unit exist, the temperature factors B_j^G have to be determined for each unit. Also, it may be the case that the displacement is not isotropic and the scalar temperature factors have to be replaced by tensors. If the dimension of a rigid unit is only a small fraction (1/5 say) of that of the whole unit cell its molecular transform is much broader than the transform of the unit cell. Thus, the diffuse background caused by random displacement of this rigid unit varies slowly from one spot to the next in an electron diffraction pattern and, therefore, can be neglected in the correction described here.

6. Conclusions

By assuming a model for the diffuse scattering in diffraction patterns from partially disordered crystals we were able to reduce the influence of diffuse background in diffraction data from 2-dimensional crystals of bacteriorhodopsin. The calculated correction, based on a crystal with trimers of bacteriorhodopsin displaced as rigid units, accounts for most of the disorder. The number of negative reflections present in the uncorrected data set decreased 4-fold to a value close to its statistical target. On average, the correction had a magnitude of 18% of the original intensities. The improvement in the data, when used for

refinement of an atomic model, lead to a marginal *R*-factor reduction of 0.40%.

Acknowledgements

The authors would like to thank Joyce Baldwin and Tony Crowther for their kind comments on the paper.

References

[1] J.M. Baldwin and R. Henderson, Ultramicroscopy 14 (1984) 319.
[2] S. French and K. Wilson, Acta Cryst. A 34 (1978) 517.
[3] T.A. Ceska and R. Henderson, J. Mol. Biol. 213 (1990) 539.
[4] R. Henderson, J.M. Baldwin, T.A. Ceska, F. Zemlin, E. Beckmann and K.H. Downing, J. Mol. Biol. 213 (1990) 899.
[5] R.M. Glaeser and T.A. Ceska, Acta Cryst. A 45 (1989) 620.
[6] H. Jagodzinski and F. Frey, Disorder Diffuse Scattering of X-rays and Neutrons, in: International Tables for Crystallography, Vol. B, Ed. V. Shmueli (Kluwer, Dordrecht, 1993) p. 392.
[7] J.-P. Benoit and J. Doucet, Quart. Rev. Biophys., 28 (1995) 131.
[8] J.M. Cowley, Diffraction Physics (North-Holland, Amsterdam, 1975).
[9] D. Leifer and R. Henderson, J. Mol. Biol. 163 (1983) 451.
[10] R.M. Glaeser, J.S. Jubb and R. Henderson, Biophys. J. 48 (1985) 775.
[11] A.J.C. Wilson, Acta Cryst. 2 (1949) 318.